Molecular footprint of co-solvents in hydrothermal liquefaction (HTL) of Fallopia Japonica

Arturi, Katarzyna Ratajczyk; Kucheryavskiy, Sergey V.; Nielsen, Rudi Pankratz; Maschietti, Marco; Vogel, Frederic; Bjelic, Sasa; Søgaard, Erik Gydesen

Published in:
Journal of Supercritical Fluids

DOI (link to publication from Publisher):
10.1016/j.supflu.2018.08.010

Publication date:
2019

Document Version
Accepted author manuscript, peer reviewed version

Title: Molecular footprint of co-solvents in hydrothermal liquefaction (HTL) of Fallopia japonica

Author: Katarzyna R. Arturi Sergey Kucheryavskiy Rudi P. Nielsen Marco Maschietti Frédéric Vogel Sasa Bjelic Erik G. Søgaard

PII: S0896-8446(18)30330-9
DOI: https://doi.org/doi:10.1016/j.supflu.2018.08.010
Reference: SUPFLU 4353

To appear in: *J. of Supercritical Fluids*

Received date: 18-5-2018
Revised date: 9-8-2018
Accepted date: 10-8-2018

Please cite this article as: Katarzyna R. Arturi, Sergey Kucheryavskiy, Rudi P. Nielsen, Marco Maschietti, Frédéric Vogel, Saša Bjelić, Erik G. Sogaard, Molecular footprint of co-solvents in hydrothermal liquefaction (HTL) of Fallopia japonica, *<![CDATA[The Journal of Supercritical Fluids]]>* (2018), https://doi.org/10.1016/j.supflu.2018.08.010

Molecular footprint of co-solvents in hydrothermal liquefaction (HTL) of Fallopia japonica

Katarzyna R. Arturi[a,b,*], Sergey Kucheryavskiy[a], Rudi P. Nielsen[a], Marco Maschietti[a], Frédéric Vogel[b,c], Saša Bjelić[b,*], Erik G. Søgaard[a]

[a] *Section of Chemical Engineering, Department of Chemistry and Biotechnology, Aalborg University Esbjerg, Niels Bohrs Vej 8, 6700 Esbjerg, Denmark*
[b] *Bioenergy and Catalysis Laboratory, Energy and Environment Division, Paul Scherrer Institut, Switzerland*
[c] *University of Applied Sciences Northwestern Switzerland (FHNW), 5210 Windisch, Switzerland*

Abstract

The influence of co-solvents on hydrothermal liquefaction (HTL) of Fallopia japonica was studied as a function of temperature. Combination of low and high-resolution mass spectrometry with multi-layered data mining strategy resulted in a comprehensive characterization of the reaction products, mostly water-soluble organics (WSO) with a broad spectrum of chemical functionalities. The non-targeted analysis revealed the presence of a core composition in the samples independent of the process conditions and consisting of hydroxycarboxylic acids, imids, lactones, lactams, phenolics, various short-chain oxygenated aliphatics, and cyclohexane derivatives. Changes in process conditions did not affect those species showing that a part of the HTL product is not susceptible to process tailoring by addition of co-solvents. The findings indicated that the effect of tetralin is a combination of solubilization and scavenging resulting in an increased abundance of monomeric aromatics. For acetone, the results pointed to the promotion of retro-aldol splitting yielding low molecular weight oxygenates.

Keywords: Acetone, Tetralin, Hydrothermal liquefaction, Fallopia japonica, Multivariate data analysis, Kendrick mass defect

2010 MSC: 00-01, 99-00

1 Introduction

Hydrothermal liquefaction (HTL) is a thermochemical technique for the depolymerization of biomass feedstocks into fuels and chemicals by means of near- or supercritical water (T_{cr} = 374 ℃, p_{cr} = 22.1 MPa) [1]. The method is versatile in terms of feedstocks, does not require biomass drying, and it takes place in a benign and environmentally friendly solvent with easily adjustable properties [2]. Currently, HTL is on the technology readiness level 5 (TRL5) with the method tested on a pilot scale [3, 4] and an

*Corresponding author, Laboratory for Bioenergy and Catalysis, Energy and Environment Division, Paul Scherrer Institute, 5232 Villigen PSI, Switzerland, Tel. +41 56 310 52 26, +41 56 310 56 15, e-mail: kasia.arturi@psi.ch, sasa.bjelic@psi.ch.

upcoming demonstration plant (TRL 6-7) [5]. The focus of HTL, and most modern commercial biorefinery concepts, lies on the production of low-carbon footprint alternatives for transportation fuels, mainly road diesel, marine, and jet biofuels. Liquid energy carriers produced from biomass are an attractive biorefinery goal because their expansion would curb the use of petroleum and thus mitigate the overall CO_2 emissions from the transportation sector, by far the worst environmental polluter. In a recent study by Pedersen et al. [6], it was shown that renewable transportation drop-in fuels from lignocellulosic biomass can be produced through hydrothermal liquefaction and upgrading for approx. 0.82-1.14 $/GLE. It has been argued that the economic viability of all biomass conversion processes in general, and HTL in particular, could be increased further by a co-production of high-value chemicals. This concept originated from the petroleum industry, where the petrochemicals represent a significant portion of the industry's overall value chain despite their relatively low volume output [7, 8]. Researchers have studied conversion of biomass into monomeric building blocks, key platform intermediates, and fine chemicals by a plethora of biological and thermochemical conversion techniques with varying degree of success. The focus today is on high-value aromatics from lignin and sugars, furfural, and 5-hydroxymethylfurfural from lignocellulose, but numerous other pathways have been proposed [9], including thermochemical routes. Chemicals of interest from HTL include small aliphatic oxygenates and aromatic monomers.

The two most elementary challenges associated with the concept of hydrothermal biomass-fueled chemical factory are poor selectivity and low yields, typically varying from 5 to 25 % [10]. While significant progress in process optimization has been achieved by tailoring with catalysts and co-solvents [9], another fundamental aspect of the problem, namely the poor understanding of liquefaction due to the lack of proper characterization of the complex products, remains to be overcome. The heterogeneity of HTL products originates from the randomness of conversion ruled by series of competing reactions including depolymerization by hydrolysis of ester and ether bonds in the biopolymers, secondary transformations of the produced monomers into intermediates, and repolymerization by condensation and cyclization, resulting in a complex product pool [11, 12]. Analysis and characterization of HTL products is therefore an area of on-going research and the most common techniques are able to describe certain fractions, e.g. gas chromatography mass spectrometry (GC-MS) covers only the volatiles. The results obtained by Bridgwater et al. [13] for products from pyrolysis specified that the content could be divided into 5-10 wt.% hydrocarbons, 10-25 wt.% oxygenated compounds (phenols, aldehydes, ketones and moderately polar alcohols), and 30-45 wt.% highly polar compounds with low, moderate, and high molecular weights. According to a similar study by Valdez et al. [14] on the composition of liquefaction products, only 10-35 wt. % of the compounds could be identified with GC-MS, with the fraction going as high as 30-50 %, in the case of co-liquefaction (HTL in water/organic solvent reaction media) as described by Biller et al. [15]. Villadsen et al. [16] concluded that the standard GC-MS is inadequate for determining highly polar compounds such as sugars and fatty acids

[17]. More advanced techniques including coupling of high performance liquid chromatography with mass spectrometry (HPLC-MS) and Fourier transform ion cyclotron resonance (FT-ICR) are under development around the world, e.g. up to 6000 individual peaks were identified by FT-ICR [18], but currently suffer from not being quantitative or only analyzing certain fractions of the HTL products. It was previously shown that a combination of novel analytical and statistical tools, such as high resolution mass spectrometry (HRMS) [19] and multivariate data analysis (MDA) [20], provides the tools needed for handling the high level of complexity of HTL products.

The focus of the current work was the development of strategies for effective and comprehensive characterization of the complex products from hydrothermal liquefaction and similar processes through the combination of standard (electron impact gas chromatography mass spectrometry, EI-GC-MS) and state-of-the-art analytical instrumentation (ultra high performance liquid chromatography coupled to high resolution mass spectrometry, UHPLC-HRMS) with customized data processing and mining techniques. The aim was to apply those tools to understand the mechanistic behavior of co-solvents in catalytic hydrothermal near-critical liquefaction of *Fallopia japonica*, an invasive plant native to East Asia, Japan, China, and Korea. Its high resilience and low requirements (fast-growing, low water input, high tolerance to a wide range of soil types, pH values, salinity, and temperature regions: above -35 ℃ [21]), would qualify *Fallopia* as an attractive lignocellulosic energy crop candidate, thus turning an environmental burden into a sustainable source of fuels/chemicals [22]. Different processes [23, 24] have already been considered for exploiting the potential of *Fallopia*, including pyrolysis [25]. Despite the fact that lignocellulosic biomass feedstocks such as *Fallopia* are generally considered too complex for modeling of an already complicated and poorly understood conversion process [26], it is important to study set-ups mimicking the real life applications of HTL for a more realistic evaluation of its potential. As shown by Carrier et al. [27] in a study comparing the conversion of biopolymers and lignocellulose, a chemical interaction between the intermediates from hemicellulose and cellulose leads to shifts in reaction pathways and thus significantly diverging final products.

The potential of *Fallopia japonica* as a biorefinery feedstock for HTL in the presence of a homogeneous catalyst (K_2CO_3) and co-solvents (acetone and tetralin) was studied as a function of conversion temperature. Both have been reported as effective tools for process optimization and product tailoring, increasing the conversion as well as selectivity [26]. Potassium carbonate was applied as a typical alkali salt catalyst promoting base-catalyzed aldol splitting of the lignocellulosic monomers [28]. K_2CO_3 was preferred over alternatives, e.g. alkali hydroxides such as NaOH, due to its low price and higher activity towards depolymerization of lignocellulosic biomass [29]. The co-solvents were selected based on their differing properties. Acetone is an aprotic polar compound, i.e. it has a lone electron pair that can accept hydrogen bonds, but it has no acidic hydrogen centers [9]. Tetralin, on the other hand, is a non-polar solvent unable of creating hydrogen bonds

nor accepting an acidic proton, but effective as a hydrogen donor [30]. Co-solvents in general are reported to increase fuel yields from HTL and to improve their properties [31] by solubilization of reaction products and scavenging of reactive intermediates [32]. A summary expanding the co-solvent effects with physical changes to the reaction system, e.g. medium viscosity, compound solubility, and ion solvation, as well as the thermodynamics of the chemical transformations, including lowering the activation energy of transient reactions, was recently provided by Shuai and Luterbacher [9]. Previous studies of acetone as a solvent and co-solvent reported reaction mechanism shifts [33] and promotion of products such as dehydroabietic acid, furans and phenolics [34] with abundant ketonic groups [35]. Part of the effect is attributed to the incorporation of the co-solvent molecule into the products by its reaction with intermediates, e.g. 3-furanmethanol to form trans-furfurylidene acetone. Tetralin as a co-solvent, on the other hand, is expected to act as proton donor promoting reduction of the reactive intermediates, an effect shown for both the liquefaction of coal [36] as well as biomass [37]. He et al. [33] demonstrated that while non-polar co-solvents such as tetralin have little effect on the conversion itself, they offer a simple and effective polarity-based measure for functioning the HTL products resulting in a purely liquid fraction more suitable for hydro-treating than the mixed aqueous/semi-solid product obtained without co-solvent. Both acetone and tetralin are interesting, yet relatively unexplored co-solvent candidates for product tailoring in HTL.

2 Materials and Methods

2.1 Materials

The biomass used in this study was a freshly harvested *Fallopia Japonica*, both leaves and branches. The plants were cut into smaller pieces, dried in an oven at 105 ℃ for 24 h, ground down to a particle size of 100 μm, dried again at the same conditions, and milled further into particles of roughly 10 μm in diameter. The inorganic content of biomass included 2 wt.% water and 5 wt.% ash (dry basis). The elemental composition was distributed as follows: 49 wt.% carbon, 7 wt.% hydrogen, 43 wt.% oxygen, 0.9 wt.% nitrogen, and 0.1 wt.% sulfur (on a water and ash-free basis). All used chemicals were obtained from Sigma Aldrich. The following organic solvents and co-solvents were used: acetone (AC, ACS reagent, $\geq$ 99.5 %), diethyl ether (DEE, $\geq$ 99.5 %), and tetralin (T, $\geq$ 99.5 %). Bromobenzene was used as an internal standard for the GC-MS analysis (IS, $\geq$ 99.5 %). K_2CO_3 (anhydrous, free-flowing, Redi-Dri^{TM}, $\geq$ 99 %) was used as a catalyst. Sodium carboxymethyl cellulose (CMC, MW approx. 250 000 g/mol) was employed as a dispersing agent (0.1 wt.%). Although CMC is an artificial carbon source, it is necessary for stabilization of the slurry and prevention of biomass sedimentation. Since CMC is expected to behave similarly to cellulose at hydrothermal conversion conditions, it is considered an appropriate measure for laboratory HTL applications [3]. Distilled water was the primary reaction solvent. N_2 (99.9 % pure) was applied for purging of oxygen from the reactor system.

2.2 Equipment and procedure

Liquefaction experiments were performed in a batch reactor designed to study biomass conversion in a highly controlled environment (accurate temperature, pressure, and reaction time values), as described in detail elsewhere [38]. Shortly: A 99 mL reactor equipped with a magnetic stirrer and a temperature control system was connected to two hand-pumps enabling injection of biomass slurry into a pre-heated and pre-pressurized environment, as well as fine pressure control through small injections/withdrawals of the reaction fluid. Fast heating and quenching of reaction products resulted in a precise control of the reaction time at the desired reaction temperature. A process and instrumentation (P&I) scheme for the system is provided in the Supporting Information (Figure S10). The study was based on a full factorial experimental design consisting of 12 runs each containing 2.5 wt.% *Fallopia* and 1 wt.% K_2CO_3 with variations of temperature (280, 300, 320 ℃) and co-solvents (A: 0 or 1 wt.% and T: 0 or 1 wt.%). The mass fractions are expressed in terms of the final composition of the reaction mixture, combining the pre-heated water/solvent and the injected biomass slurry inputs. The runs were performed in a random order to ensure the statistical independence of the obtained results. The experimental procedure was as follows: a 45 g mixture of water, K_2CO_3, and co-solvent was injected into the reactor with one of the two hand-pumps; the reactor was purged with N_2 and heated up to a temperature 30 ℃ above the desired reaction temperature with pressure rising simultaneously slightly above the saturation pressure at any given temperature. A feed slurry containing biomass, water, K_2CO_3, and CMC was mixed using an IKA Ultra Turrax (30 min, 20000 rpm) and then injected through the second pump until the desired pressure was reached (190, 220, and 250 bar for 280, 300, 320 ℃, respectively). The composition of the reaction mixture was calculated based on the desired reaction conditions and the pre-heated mixture taken into account. The final concentrations are summarized in Table 1. The injection of biomass slurry resulted in a small pressure and temperature drop followed by an immediate increase up to the target values. The heating and pressure profiles for the system are presented in Figure S11 (Supporting Information). After the reaction time (τ = 10 min), the products were rapidly depressurized and cooled down in a cold trap. The gas products were not collected.

2.3 Analytical strategy

Once the reaction mixture was cooled down to room temperature, the products were separated by centrifugation (6000 rpm, 4 hr) into aqueous (top) and non-aqueous semi-solid (bottom) fractions. The top fraction containing water soluble organics (WSO) was analyzed after preparation steps required by the specific analytical instrumentation. The analysis included total organic carbon analysis (TOC: AI-Analyzer Multi N/C 2100S with pO_2 = 5 bar, flow O_2 = 160 ml/min, and T_{oven} = 800 ℃, preparation: dilution and filtration), as well as a detailed characterization of the organics by coupling of chromatography and spectrometry (see Subsections 2.4 and 2.5 for specific details). The bottom fraction was additionally separated into a lighter, acetone soluble phase, and a solid char phase (separated by filtration under vacuum,

Whatman No. 5). The char fraction was assessed exclusively with regard to its carbon content (Perkin Elmer 2400 Series II CHNS analyzer) after drying in an oven at 105 ℃ overnight. The extraction of the water insoluble organics (WIO) took place by evaporation of the solvent (vacuum at T = 35 ℃ and p ≈ 500 mbar). WIO samples were prepared and characterized in detail correspondingly to the WSO, except for its carbon content, which was determined by the CHNS-O analyzer instead of TOC. The C-inputs for carbon balances into the reactor included biomass, co-solvents, CMC, and K_2CO_3, while the carbon outputs combined the organic and inorganic C in the aqueous phase (determined by total carbon, TC, measurements), WIO, and char (both determined by elemental analysis). The moisture content and the ash content in the biomass, char, and the WIO were determined thermogravimetrically (TGA, N_2 flow 35 cc/min, heating 10 K/min from 25 ℃ to 110 ℃). The separation procedure after HTL and analytical strategy used for characterization of different product fractions are summarized in Figure S12 in the Supporting Information.

2.4 SPME-GC-MS

The sampling method before GC-MS was optimized for each fraction: solid-phase microextraction (SPME) for WSO [39] and liquid-liquid extraction (LLE) for WIO. The SPME equipment used in this study (manual sampling holder with needles 23 gauge and 65 μm poly(dimethylsiloxane) divinylbenzene PDMS/DVB adsorbent fiber) were purchased from Supelco (Bellefonte, PA, USA). The fibers were conditioned daily in the GC injector according to the recommendations of the manufacturer (30 min at T = 250 ℃) before use. In between the runs, the fiber was cleaned (10 min at 225 ℃), and a possible carry over was assessed by a blank run. A set of 15 initial extractions was used to develop an optimal SPME extraction procedure (extraction temperature, time of extraction, presence of salt, pH changes). The aim was to increase the partition coefficients and decrease the time required for obtaining equilibrium. Based on the results, the variation of pH (below 2 and above 10) was the only factor with no tangible influence on the extraction results. The final optimized method maximized the concentration of the volatile components in the head-space. A sample (5 ml of the water phase) was placed in a 22 ml glass vial containing a magnetic stirrer, 50 mg of internal standard solution (IS) and 1 g of NaCl were added and the vial was sealed using a PTFE coated silicone rubber septum. The vial was placed in a thermostated bath adjusted to T = 50 ℃. The fiber was exposed to the head-space (HS) of the sample for 10 min. After the sampling, the SPME fiber was retracted into the syringe, injected through the septum into the GC, and desorbed for 1 min. The apparatus used for gas chromatography mass spectrometry was a Perkin Elmer Clarus GC 580 and MS SQ 8 S with EI and a quadrupole ion analyzer. A Perkin Elmer Crossbond column (30 m x 0.25 mm ID, 0.25 μm 95 % dimethyl polysiloxane and 5 % biphenyl) with helium as a carrier gas (1 ml/min) was used to separate the analytes. For SPME, the analytes were desorbed at T = 200 ℃ in a split mode (50:1) with 1 min solvent delay. The GC-MS program was optimized for the applied SPME fiber (T = 40 ℃ hold for 2 min followed by a heating ramp of 10 K/min to T = 200 ℃ hold for 2 min). WIO samples were extracted

with DEE (1:1), injected at T = 300 ℃ in split mode (30:1) with solvent delay of 2.5 min, and heated (T = 75 ℃ held for 1.5 min followed by a heating ramp of 10 K/min to T = 275 ℃ held for 10 min). MS spectra were recorded at 70 eV ionization energy and scanned for m/z 75 - 600. The main components were tentatively identified by the NIST 11 database.

2.5 UHPLC-HRMS

The WSO and WIO samples were analyzed directly and diluted 1:1000 in a solvent mix (1:1:1:1 vol.% of methanol, acetone, toluene, and chloroform), respectively. Prior to the analysis, the solutions were filtered (0.22 μm). Carry-over was assessed by a blank run in between each analysis. The injection was 1 μl and 10 μl in the case of aqueous phase with WSO and the WIO dissolved in the solvent mix, respectively. The time-resolved separation of the analytes was performed in a Thermo Scientific Dionex^{TM} Ultimate 3000 Series RS system (Thermo Scientific^{TM}, Switzerland) including a pump, a column compartment, and an auto-sampler. The used column and pre-column were Thermo Scientific^{TM} Accucore^{TM} RP-MS (150 mm x 2.1 mm, particle size 2.6 μm). The following program with mobile phase A (1 vol.% methanol, 1 vol.% acetonitrile and 0.2 vol.% HCOOH in high purity water) and mobile phase B (100 vol.% MeOH) was applied: 1 % B (0-1 min) 1 to 99 % B (1-6 min), 99 % B (6-8 min), followed by equilibration step and 99 to 1 % B (8-8.2 min), 1 % B (8.2-10 min). The flow was set to 0.7 ml/min, the temperature of the column was kept constant at T=50 ℃. A heated electrospray ionization (ESI, 3.5 kV spray voltage) in positive and negative mode was used for the ionization of the analytes. Data acquisition was performed using Thermo Scientific^{TM} Q-Exactive^{TM} hybrid quadrupole-orbitrap mass spectrometer controlled by Xcalibur 4.1 software. Mass spectra were acquired in full scan mode with an isolation window of 1 m/z from 50-750 m/z. The resolution was 70'000 at m/z = 200. Raw mass spectral data files were collected in triplicate including a blank between each run.

2.6 Data Processing and Mining

The UHPLC-HRMS data were imported into Compound Discoverer^{TM} 2.1 software (Thermo Scientific^{TM}, Switzerland) and processed with standard settings except for mass tolerance (set to 2.5 ppm). Chromatographic peaks detected in one of the input files but missing in others were checked by "Fill Gaps" option. The composition (of a general formula $C_cH_hO_oN_nS_s$) was predicted based on exact mass and isotopic patterns and evaluated against MS/MS spectra. The identity of the compounds was determined where possible with mzCloud [40]. Only features yielding formulas present in ChemSpider were used [41]. Measured data and calculated features and properties of the samples were used as input to descriptive and differential statistics, as well as various non-target data screening and mining techniques including: 1) Quantification of the direction and strength of the linear association between process conditions (temperature, tetralin, acetone) and an average species' properties (aromaticity index AI, double bond equivalents DBE, molecular weight, H/C ratio, O/C ratio, N/C ratio, the number of carbon, hydrogen, nitrogen, and oxygen atoms). The

properties of the "average" species from each run were computed by weighting the features of the compound pool according to the normalized areas. Spearmann correlation coefficient was calculated with the values ranging between -1 (i.e. higher levels of one variable are associated with lower levels of the other) and +1 (i.e. higher levels of one variable are associated with higher levels of the other). More details can be found in the literature [42]; 2) Principal component analysis (PCA) was performed with the aim of mining hidden trends. PCA is a statistical procedure that uses an orthogonal transformation to convert a set of observations of possibly correlated variables into a set of values of linearly uncorrelated variables called principal components (PCs). The first principal component represents the direction of largest possible variance in the data, as do the following PCs under the constraint that they is orthogonal to the preceding components. In this study, PCA was performed directly on the raw data (ncomp = 20, no scaling, the whole GC-MS data set), as well as on the normalized peak areas (ncomp = 20, no scaling, UHPLC-HRMS, data splitted into four groups according to the product fraction and ESI polarity: WSO positive mode, WIO positive mode, WSO negative mode, and WIO negative mode). The results were evaluated by score plots (projection of the samples to the principal components) and loading plots (contribution of each variable to the orientation of the PCs) for pairs of principal components. Additional details about PCA can be found elsewhere [43]. The calculations were performed in R (version 3.2.2), a free software environment for statistical computing, supported by mdatools package [44]; 3) Volcano plots, a type of scatter-plot that is used to quickly identify changes in large data sets composed of replicate data [45], were used to visually identify statistically significant differences between the abundances of the molecular species detected in two different samples, e.g. A0T0280C and A0T0300C (the influence of temperature in the absence of co-solvents). The plots show the $\log_2$ of fold-change on x-axis as a function of the statistical significance ($-\log_{10}$[p-value] from a post-hoc ANOVA analysis) on the y-axis. The terms down-regulated, non-affected, and up-regulated are used for species whose abundance decreased, did not change, and was increased, respectively. The analysis was used to assess the number of species affected by perturbations in the process parameters, as well as to create groupings of species used in the subsequent analysis; 4) Analysis and comparison of the samples' hydrogen and oxygen contents by van Krevelen plots, a graphical-statistical method demonstrating the oxygen:carbon ratios as a function of hydrogen:carbon ratios of the detected compounds as proposed by van Krevelen [46]. The method provides a handy non-targeted assessment of hundreds of chemical species in a complex mixture [47]. H/C and O/C ratios for WSO and WIO were plotted for all runs separately, in addition to the differential van Krevelen plots focusing on the differences in the hydrogen:carbon and oxygen:carbon ratios obtained by varying the temperature and co-solvents within the classes defined by volcano plot analysis. In addition, the data points were colored according to their aromaticity index as proposed by Koch and Dittmar [48]; 5) Kendrick plots showing the nominal Kendrick mass (NKM) as a function of Kendrick mass defect (KMD) was used to group homologous series of species. The Kendrick mass is defined by setting the mass of a chosen molecular fragment, in this case CH_2, to an integer value in atomic mass units, here

14 (1xC+2xH=1x12+2x1=14). The advantage of this method is that species belonging to a homologous series will be positioned on a horizontal line due to identical mass defects, thus providing a compact visual analysis. KMD method is a common tool for high-resolution mass spectra as is described in detail elsewhere [49]. Kendrick mass and Kendrick mass defects were calculated as follows:

$$\text{Kendrick exact mass} \approx CH_2 = \text{Observed exact mass x } \frac{14.00000}{14.01565}$$

$$\text{Kendrick mass defect} = \text{Nominal mass} - \text{Kendrick exact mass}$$

3 Results

3.1 Carbon balances

The trends of the HTL of *Fallopia japonica* at different conditions were assessed by means of carbon distribution in the product fractions (Figure 1). The carbon distribution highlights the masses of carbon ending up in a given fraction (WSO, WIO, or char, excluding gas and losses) divided by the total mass of carbon retrieved in the analyzed products. Overall, high total (based on the carbon input from biomass) recoveries of carbon were obtained in the absence of co-solvents (108 ±4 wt.%), showing a good control over the process' mass flows in the designed experiential procedure. In the presence of co-solvents, additional losses were observed due to the evaporation of the volatile co-solvents and reaction products. Independently of the process conditions, WSO was the most significant fraction of the products (WSO_{avg}=70 wt.%, WSO_{min}=48 wt.%, WSO_{max}=86 wt.%), due to the combination of a low biomass input, short residence times, and the presence of solubilizing co-solvents. The formation of WSO is also typically favored at low homogeneous catalyst/biomass ratios (< 0.5 in the current study) as reported by Rustamov et al. [50]. Largest WSO carbon pools were obtained in the absence of co-solvents and with acetone (76 ±12 wt.%, 76 ±3 wt.%, and 61 ±13 wt.% for A0T0, A1T0, and A0T1 respectively). When tetralin was present, the flow of carbon shifted towards WIO (31 ±9 wt.% for A0T1 and 24 ±3 wt.% for A1T1 vs. 16 ±5 wt.% for A0T0 and 17 ±3 wt.% for A1T0). The used acronyms are explained in Table 1. From this evidence alone, it is not possible to determine whether the effect was due to a change in mechanism or the solubilization effect, i.e. incorporation of the reaction products into the phases corresponding to the co-solvents' polarity. The deviation values represent the variation between different temperatures. At low temperatures, the production of char was significant (17 ±3 wt.% at T=280 ℃ vs. 4 ±3 wt.% and 4±2 wt.% at T=300 ℃ and T=320 ℃, respectively). The flow of carbon shifted from the char towards WSO and WIO with temperatures rising from T=280 ℃ to T=300 ℃, indicating a boost in biomass conversion.

3.2 Characterization of WSO and WIO volatiles by GC-MS

The quality of the tentative identifications obtained from the NIST library for the detected GC-MS species were evaluated in terms of match probability, compounds' molecular weights, boiling points, and

their abundance in the HTL-related literature. In the aqueous fraction, approx. 50 WSO species from the pool of 150 detected peaks were assigned an acceptable match versus an average of 15/50 (identified/detected) compounds per run for WIO. The relatively low number of detected peaks and identifications conforms with previously reported HTL results. According to Liu and Zhang [34], water based liquefaction yields the smallest fraction of GC-MS identifiable products, with 44 vs. 57 species liquefied in water and water/organic co-solvents mixtures, respectively. *Fallopia* was converted into a mixture of oxygenated organics: low molecular weight oxygenates (LMW, 0-1 %), cyclic carbonyl compounds (10-22 %), aromatics (57-81 %), and repolymerization products designated here as higher molecular weight species (HMW, 8-26 %). While depolymerization of lignin in addition to dehydration of glucose were the main sources of the aromatic compounds [51], the origin of cyclics is more uncertain. The presence of cyclopentanone derivatives indicated a pathway involving hydrogenation of furans. Similar products were reported previously in the literature [52]. The effect of conversion conditions on the production of volatiles from HTL was assessed by the product distributions (Figure S13 in the Supplementary Information). According to the results, in the absence of tetralin, cyclics and HMW classes were more abundant, while in its presence, the conversion pathways shifted towards aromatic WSO. Similar findings have been reported previously for the HTL of lignocellulose in the presence of small polar co-solvents [34]. According to the GC-MS results, the volatile WIO fraction was constituted mainly of short-chained alkanes and alkenes, semi-polar aromatics, and repolymerized structures. A list of the top 10 most common WSO and WIO chemicals identified by GC-MS is compiled in Table S2 in the Supplementary Information.

A further evaluation of the SPE-GC-MS data obtained for WSO was performed by application of PCA, a simple eigenvector-based multivariate method for exploratory assessment of large data sets such as chromatographic and spectrometric data [53]. In this method, the original data is projected onto a set of orthogonal vectors called principal components (PCs). PCs are uncorrelated with each other linear combinations of the original variables oriented along the directions of maximum spread of the data points. This method allows to reduce the complexity and dimensionality of the data, thus increasing interpretability and minimizing information loss [54]. It also allows to find hidden structures in the objects relationship, such as groups, trends, and outliers. The results of PCA were evaluated with score and loading plots. A score plot is a scatter plot, which shows the projection of data objects (samples) to the principal components (so every marker/point on this plot represents a particular sample/measurement). A loading plot shows contribution of each variable (chromatographic peak) to the orientation of the corresponding component. Objects (samples) positioned close to each other on a score plot are considered similar according to the variable (a peak or a group of peaks) dominating the corresponding loading. Markers on the score plots were color coded according to the conversion conditions (temperature, acetone, and tetralin). This resulted in a discovery of a hidden trend related to the presence of tetralin (Figure 2) explained by PC1 responsible for more than

67 % of the total variability between the groups with and without tetralin, respectively. The tendency was traced to the increasing abundances of anisole (A), cresol (C), methylhexahydroindenone and trimethylhexahydroindene (I), and dihydroeugenol (E) in the samples produced with (A and C) and without (I and E) tetralin, respectively. Anisole and cresol are typical final lignin conversion products, dihydroeugenol is an intermediate, and the indene/indenones are repolymerized structures [55]. The obtained results indicated that tetralin as a co-solvent facilitates the conversion of lignin from lignocellulose into monomeric aromatics and prevents repolymerization by acting as a capping agent for reactive species, similarly to the effect of phenol as a co-solvent [38]. However, opposite to the application of phenol, the tetralin molecule was not incorporated into the reaction products, as its scavenging effect was most probably realized through hydrogenation of the reactive intermediates. The effect of hydrogenation was indicated with the presence of dihydroeugenone, which originated from dehydration and H_2 addition to known lignin depolymerization products e.g. coniferyl alcohol.

3.3 Characterization of semi- and non-volatiles by UHPLC-HRMS

3.3.1 Molecular features

A full MS scan combined with tandem MS/MS scans of the most significant peaks allowed a comprehensive assessment of the samples' composition with a high level of identification confidence as defined by Schymanski et al. [56]. In all, 2407 and 1017 species were detected and assigned a sum formula among WSO and WIO, respectively. The distribution of the species' selected features, including their molecular weight, aromaticity index, and number of carbon atoms, are shown on Figure 3. HTL of *Fallopia* resulted in a rather narrow spectrum of reaction products with molecular weights ranging from 50 to 800 g/mol, low aromaticity index values, and n=8 as the average number of carbon. An examination of the correlation between the process parameters and an average species' features (aromaticity index AI, double bond equivalents DBE, molecular weight, H/C ratio, O/C ratio, N/C ratio, the number of carbon, hydrogen, nitrogen, and oxygen atoms) weighted according to the normalized areas resulted in Figure 4. According to the findings, conversion temperature was correlated inversely to the oxygen content of the reaction products, i.e. at high reaction temperatures, the average species typically contained fewer oxygen atoms. While the presence of acetone did not exhibit statistically significant effects, tetralin affected AI, DBE, along with lowering the number of C and H, but increasing the O/C ratios. The decreasing polyaromaticity, lower degree of unsaturation, and the size of the molecules were all indicative of preventing repolymerization through protonation of reactive intermediates.

3.3.2 Mining of trends

Additional exploration of the general trends in the data was performed by PCA of the normalized chromatographic peak areas obtained from the UHPLC-HRMS measurements. A multivariate approach

corresponding to the SPE-GC-MS analysis was applied. The data was analyzed as a whole, as well as in groups. The results were assessed by the means of scores (projection of the samples) and loading plots (contribution of each chromatographic peak to the orientation of the PCs). While the results from the entire data set were unclear and did not yield unambiguous trends, further insight was gained from the analysis of the data grouped according to the ESI mode (positive and negative) and product fraction (WSO and WIO). On average, no more than five principal components (PCs) were enough to explain more than 90 % of the data variance. The most distinctive trends were discovered for the WSO in the positive mode, where the changes in temperature were represented by PC1 and explained 47 % of the variation in the data (Figure 5). Additionally, the presence of acetone was explained by a grouping according to PC2 (18 %). The loadings were used to identify the molecular species responsible for the remarkable separation of the samples. While with increasing temperatures repolymerized structures were promoted at the expense of small molecular weight species and monomers such as dimethoxyphenol (Table S3 in the Supplementary Information), the presence of acetone resulted in an increased abundance of short-chain aliphatic oxygenates (e.g. heptadienal) and suppression of cyclic compounds. The corresponding analysis of WIO did not yield unambiguous trends or clear patterns. In most of the analyzed WIO cases, the loadings responsible for the trends encompassed a large group of chemical species rather than single compounds.

3.3.3 Statistically significant perturbations

The statistical validity of perturbations between different runs was assessed by means of volcano charts, which plot $\log_2$ of the fold-change on the x axis versus significance ($-\log_{10}$ of the p-value from a post-hoc ANOVA analysis) on the y axis. The fold change was calculated as the ratio of the peak area from one run (A_1) and the peak area from a second run (A_2), e.g. $(A_1)/(A_2)$. The abundance of different chemical species was analyzed by comparing the intensity of the signal for different m/z values. Statistically relevant changes in the composition can be found away from the central line ($log_2 < -2 \wedge 2 < log_2$) representing the zero fold change and at the top of the plot representing the lowest p-values (p-value<0.005). Figure 6 shows examples of the produced volcano plots with significantly down-regulated, non-affected, and up-regulated populations of molecular species for pairwise comparisons of the runs. The terminology down-regulated, non-affected, and up-regulated was used for species whose abundance decreased, did not change, and was increased significantly, respectively. See Section 2.6 for more details. Figure S14 in the Supplementary Information summarizes the combined number of WSO and WIO species in each group and for each set of runs. Most significant down-regulation of the number of species took place in the presence of acetone going from 300 to 320 ℃. Several condition sets resulted in significant up-regulation of the chemical species, most notably by increasing the temperature from 280 to 300 ℃. Even more importantly, the results revealed that a significant fraction of the HTL products remained unaffected by the varying reaction conditions, which indicated that tailoring and optimization influences only a susceptible part of the intermediates, while a

core of conversion products depends only on the supply of minimum activation energy. The results were confirmed by van Krevelen plots (Figures S15-S17 in the Supplementary Information). According to these findings, saturated and unsaturated aliphatics (H/C ratio >1) were the most common constituents of the HTL products. Molecules on vertical lines differ by their amount of hydrogen. Molecules on horizontal lines differ by their content of oxygen. Oxygen containing aliphatics were predominant among the WSO (0< O/C ratio<1), while the O-content in WIO was significantly lower (the majority 0< O/C ratio <0.3). The vertical line representing the O/C ratio of 0.0 and thus oxygen-free species was most prominent among the aromatic and aliphatic WIO species. The hydrogen:carbon ratios were, on the other hand, much more broadly distributed in WIO than in WSO (0.5< H/C ratio <2.5 vs. 1< H/C ratio <2, respectively). Figure 7 shows the differential van Krevelen plots with the data points classified according to the volcano results (up-regulated, non-affected, down-regulated) for the influence of temperature and the presence of co-solvents. The majority of the species fell in the "non-affected" category and only few compounds were affected by the perturbations in the reaction conditions.

3.3.4 Identification of compounds

From the pools of species with a molecular formula, the most significant compounds were selected based on a defined peak area threshold (295 and 103 molecules in the positive and negative mode, respectively) and a number of peaks was identified unambiguously (99 and 62 molecules in the positive and negative mode, respectively) by searching mzCloud database [40]. A summary outlining the top 20 most abundant compounds in the data set is presented in Table S4 in the Supplementary Information. Species related to the co-solvents autonomous conversion under hydrothermal conditions were identified as well. 3,3,6,8-Tetramethyl-1-tetralone was formed as the result of acetone self-condensation reactions taking place at increased temperatures and in the presence of alkali [57] and involving: 1) aldol condensation of acetone to diacetone and triacetone alcohol; 2) dehydration of triacetone alcohol to phorone; 3) 1,6-Michael cyclization of phorone to isophorone; 4) condensation of isophorone with mesityl oxide (formed by dehydration of diacetone alcohol) [58]. In the case of tetralin, both dihydronaphthalene and naphthalene were identified among the reaction products.

The data points with areas above the defined threshold were classified according to the volcano results (non-affected core, up- and down-regulated), and the core species were processed by the Kendrick mass defect (KMD) method, in which the species' KMD values are plotted as a function of their nominal Kendrick mass (NKM). According to the results in the negative ESI mode outlined in Figure 8, α-hydroxycarboxylic acids were the most abundant species in addition to imids (two acyl groups bound to nitrogen) and lactones (cyclic esters of hydroxycarboxylic acids). Carboxylic acids, which are valuable intermediates and fine-chemicals used widely in the food, chemical, and material industries, were the main high-value output from HTL of

Fallopia. A traditional pathway for their formation include oxidation of alcohols (-OH) into carbonyl (=O) and then carboxyl (-COOH) functional groups. Numerous authors have reported the formation of acids through retro-aldol splitting of glucose and fructose to glyceraldehyde, oxidation to puryvaldehyde, and finally to formic acid, lactic acid, and acetaldehyde [59]. It should be mentioned that glyceraldehyde can be reversibly converted into dihydroxyacetone, crossing the biomass conversion pathways with transformations of acetone under hydrothermal conditions. Other authors reported the presence of acids such as acetic acid, propionic acid, and glycolic acid [60, 61]. Long chained carboxylic acids (e.g. hexadecanoic acid) have been previously reported in the products from HTL due to the hydrolysis of glycerides [16]. No studies to date have reported the formation of C4-C7 hydroxy- and dicarboxylic acids from HTL, and their exact origin is uncertain, although it can be speculated that they were produced by carboxylation and molecular skeletal rearrangements of C5 sugars (e.g. xylose, arabinose, and lyxose) from hemicellulose producing e.g. ascorbic acid [62]. In the positive mode, the core composition comprised a mixture of aliphatic, cyclic, and aromatic species with a broad spectrum of chemical functionalities, e.g. lactams, phenolics, short-chained unsaturated oxygenates, cyclohexane derivatives, and β-hydroxycarboxylic acids. In addition to visualizing the composition of the core HTL products, KMD analysis was also used to identify species according to their position on a horizontal line representing homologous series. An example includes the identification of the last data point on the first horizontal line in the top part of Figure 8 as hydroxyheptanioc acid, a C7 hydroxycarboxylic acid in a homologous series starting with glycolic acid.

The influence of co-solvents on the conversion was studied further by examination of statistically significant effects in pairwise comparisons of the species' abundance (e.g. A1T0280 vs. A0T0280, A0T130 vs. A0T1300). The results showed that while numerous statistically significant differences in composition related to variations in reaction conditions could be identified, no generally valid trends were present (Table S5 in the Supplementary Information). These results do not represent any general trends in the data, but are rather an one-on-one comparison of the effects. Overall, acetone caused shifts in the aromatic monomer balances, e.g. it suppressed the yields of dimethoxyphenol and favored methoxysalicylic acid, possibly by the increased hydrolysis of the former into the latter. Carboxylic acids were not universally favored in the presence of acetone as the yields of compounds such as benzoic, homovanillic, and hydroxycinnamic acid were lower with the co-solvent than without it. In the case of tetralin, aliphatic acids were promoted alternative to aromatic acids. Common for both co-solvents was the favorable formation of aromatic-cyclic dimers, e.g. phenylcyclohexanedione.

4 Conclusions

In the current work, *Fallopia japonica*, an invasive species of weed and a potential lignocellulosic energy crop, was depolymerized hydrothermally at varying temperatures in order to explain the influence of acetone and tetralin co-solvents on the conversion and product formation. An illustration of the reaction trends at different conditions for biomass conversion clarified by the data mining approach is presented in Figure 9. The major part of the product consisted of WSO. A result obtained by a combination of low biomass loading and short reaction time. Addition of tetralin resulted in a partial shift of carbon from WSO towards WIO, most probably through the solubilization of the less polar reaction intermediates in the co-solvent. A combination of standard (GC-MS) and state-of-the-art (UHPLC-HRMS) analytical instrumentation, as well as a non-targeted data mining strategy, resulted in a comprehensive characterization of both WSO as well as WIO covering molecular species with wide-ranging volatilities, molecular weights, and polarities. While according to GC-MS, aromatics were the most common HTL conversion products, UHPLC-HRMS pointed towards short-chain oxygenated aliphatics with a broad spectrum of chemical functionalities. Application of GC-MS alone would not allow the identification of e.g. α-hydroxycarboxylic acids, which constituted the core composition of the obtained HTL products. Carboxylic acids, which are valuable intermediates and fine-chemicals used widely in the food, chemical, and material industries, were the main high-value output from HTL of *Fallopia*. In addition to the acids, imids, lactones, lactams, phenolics, cyclohexane derivatives, and β-hydroxycarboxylic acids were also identified. Process conditions did not affect the abundances of those species indicating that only certain parts of the products are susceptible to process tailoring and optimization. The presence of co-solvents increased the abundance of monomeric aromatics (tetralin: anisole and cresol) and small oxygenates (acetone: heptadienal) and decreased the abundance of repolymerized species (methylhexahydroindenone and trimethylhexahydroindene) and aromatic intermediates (dihydroeugenol). For tetralin, the effect was attributed to the prevention of repolymerization, most probably through hydrogenation of reactive intermediates. For acetone, the results pointed to the promotion of retro-aldol splitting resulting in low molecular weight compounds as the most important pathways for conversion following the hydrolysis of the biopolymer chains.

5 Acknowledgements

This research project is financially supported by the Swiss Innovation Agency Innosuisse and is part of the Swiss Competence Center for Energy Research SCCER BIOSWEET, the Danish Council for Strategic Research (DSF grant no. 1305-00030B), Danish Agency for Science, Technology and Innovation (grant no. 11-118412), and by Marie Curie Career Integration Grant (FP7-PEOPLE-2012-CIG, project no. 321816). Part of this work was supported by and performed within the Energy System Integration (ESI) platform at the Paul Scherrer Institute.

6 Artwork

Table 1: The composition of the reaction mixtures. The experiments were performed in a randomized order to ensure the statistical independence of the obtained data (indicated next to the label coding). A-acetone, T-tetralin, B-biomass.

Run	T (℃)	A (wt.%)	T (wt.%)	B (wt.%)	K_2CO_3 (wt.%)	CMC (wt.%)
A0T0280C (10)	280	0.0	0.0	2.49	1.07	0.12
A0T0300C (11)	300	0.0	0.0	2.33	1.09	0.11
A0T0320C (12)	320	0.0	0.0	2.19	1.11	0.10
A1T0280C (01)	280	1.00	0.0	2.20	1.07	0.09
A1T0300C (04)	300	0.91	0.0	2.31	1.11	0.11
A1T0320C (08)	320	1.11	0.0	2.29	1.09	0.11
A0T1280C (06)	280	0.0	1.00	2.49	1.10	0.11
A0T1300C (03)	300	0.0	0.93	2.31	1.13	0.11
A0T1320C (07)	320	0.0	1.07	1.97	1.09	0.09
A1T1280C (05)	280	1.01	1.02	2.46	1.09	0.11
A1T1300C (09)	300	1.02	1.02	2.33	1.08	0.12
A1T1320C (02)	320	1.01	1.07	2.12	1.12	0.10

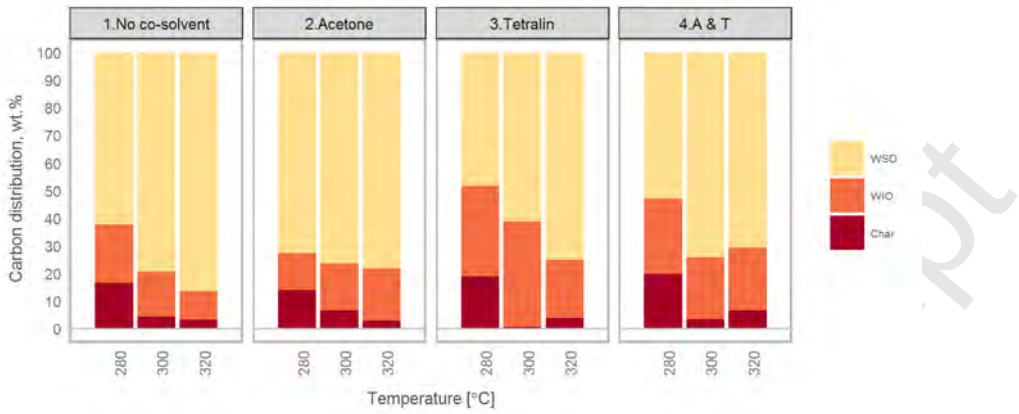

Figure 1: Distribution of carbon in the product fractions from different runs.

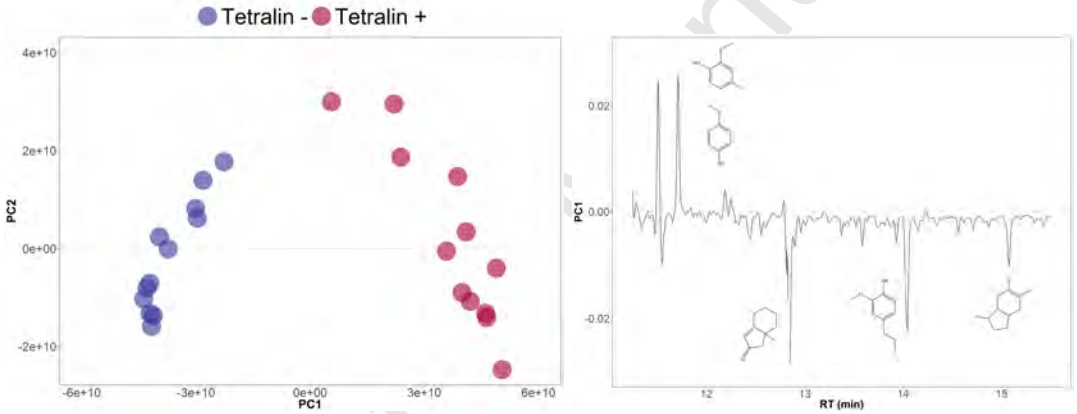

Figure 2: PC1 vs. PC2 score (left) and PC1 loading (right) line plots identifying molecular species responsible for the largest variation in the GC-MS dataset and explaining the hidden pattern and grouping between the samples produced without (blue scores, negative loadings) and with (red scores, positive loadings) tetralin as co-solvent.

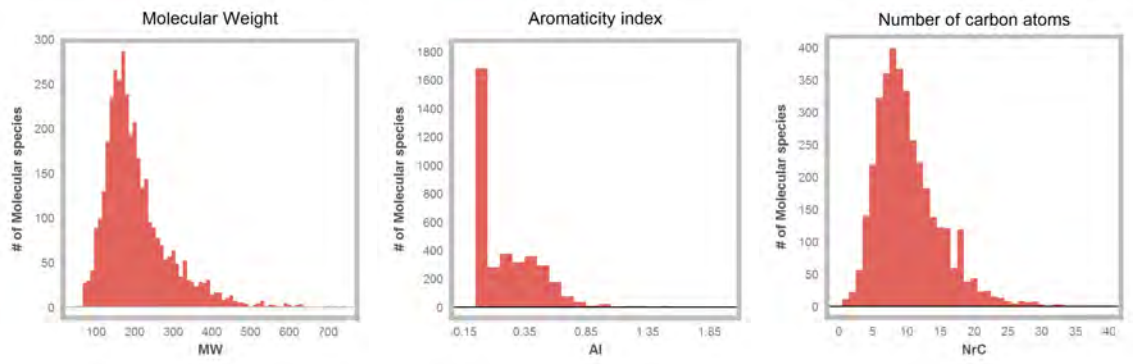

Figure 3: Selected features of the molecular species detected by high resolution hybrid quadrupole orbitrap tandem mass spectrometry. The histograms show a combined result for WSO and WIO in both positive and negative ESI ionization modes.

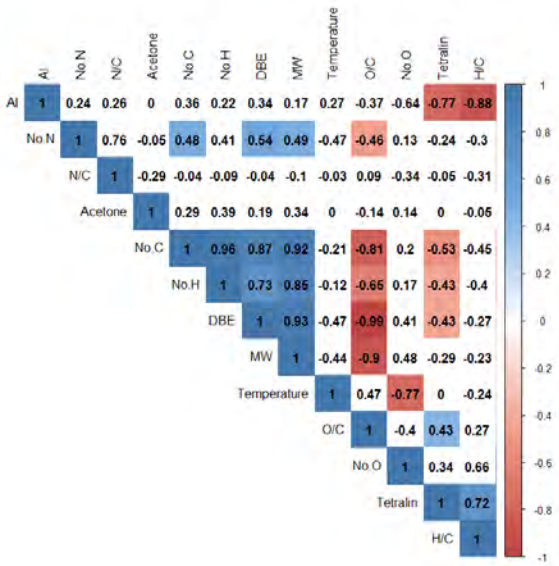

Figure 4: Spearman matrix showing the direction and strength of the linear association between process conditions and an average species' properties. Statistically significant (p-value<0.005) direction of the association are outlined in red (negative) and blue (positive) with the magnitude of the correlation coefficients indicating the strength of the association.

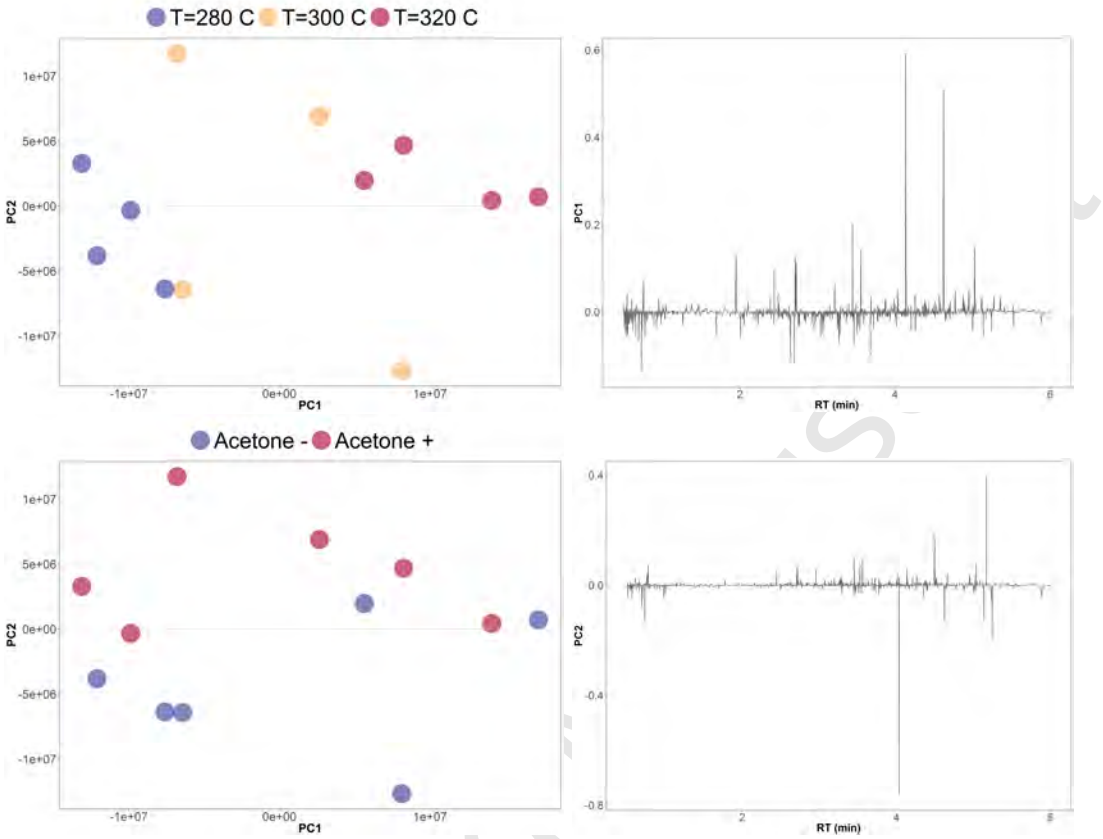

Figure 5: PC1 (46.47 %) vs PC2 (18.12 %) score (left) and PC1/PC2 loading plots (right) for WSO measured in the ESI positive mode.

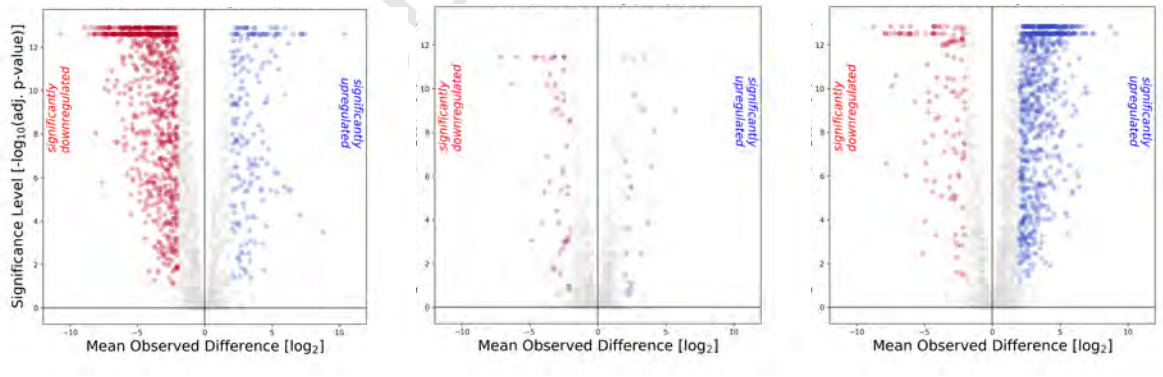

Figure 6: Volcano plots for AQ-R01: A1T0280C vs. AQ-R04: A1T0300C (temperature influence in the presence of acetone, significantly down-regulated), AQ-R05: A1T1320C vs. AQ-R10: A0T1320C (tetralin influence at T=320 ℃, non-affected), and AQ-R08: A1T0320C vs. AQ-R15: A0T0320C (acetone influence at T=320 ℃, significantly up-regulated). Note: the number of points in all graphs are equal.

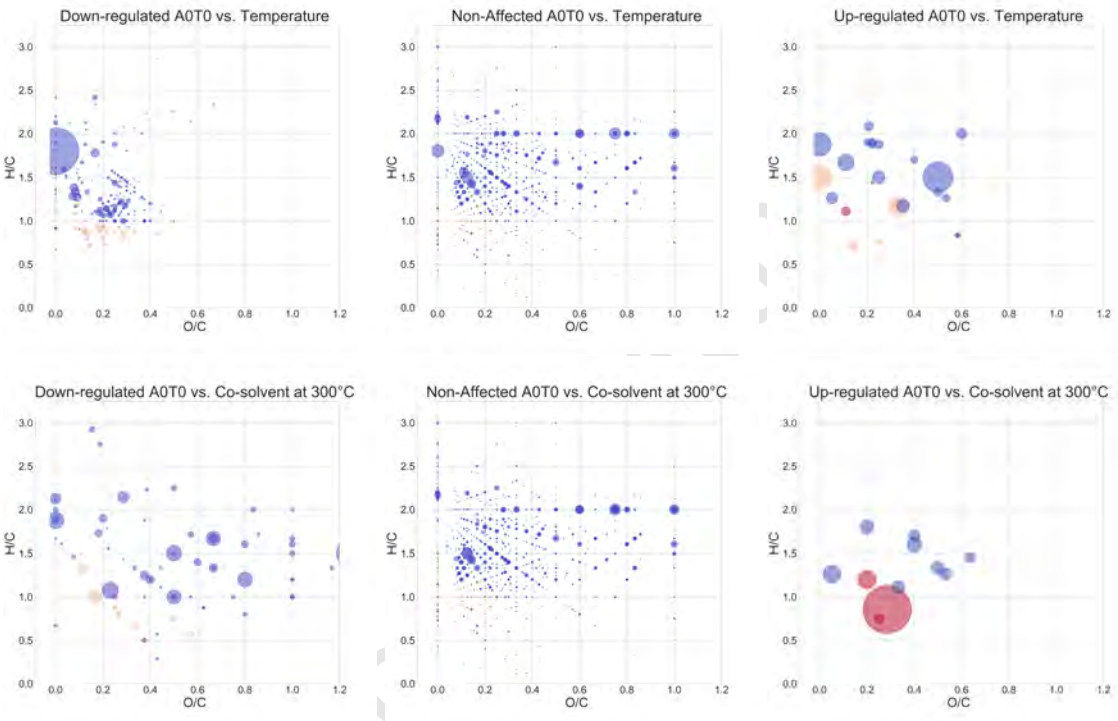

Figure 7: Differential van Krevelen diagrams combined for statistically significant changes (left: down-regulated, middle: non-affected, right: up-regulated) in WSO and WIO (combined analysis as obtained from Volcano plots) showing the differences between the samples processed at different temperatures (top) and with/without co-solvents (bottom). The data was obtained from UHPLC-HRMS. Size of the points is proportional to the area detected normalized by sum. The color code varies according to the aromaticity index: blue - aliphatic, orange - aromatic, red - condensed aromatics.

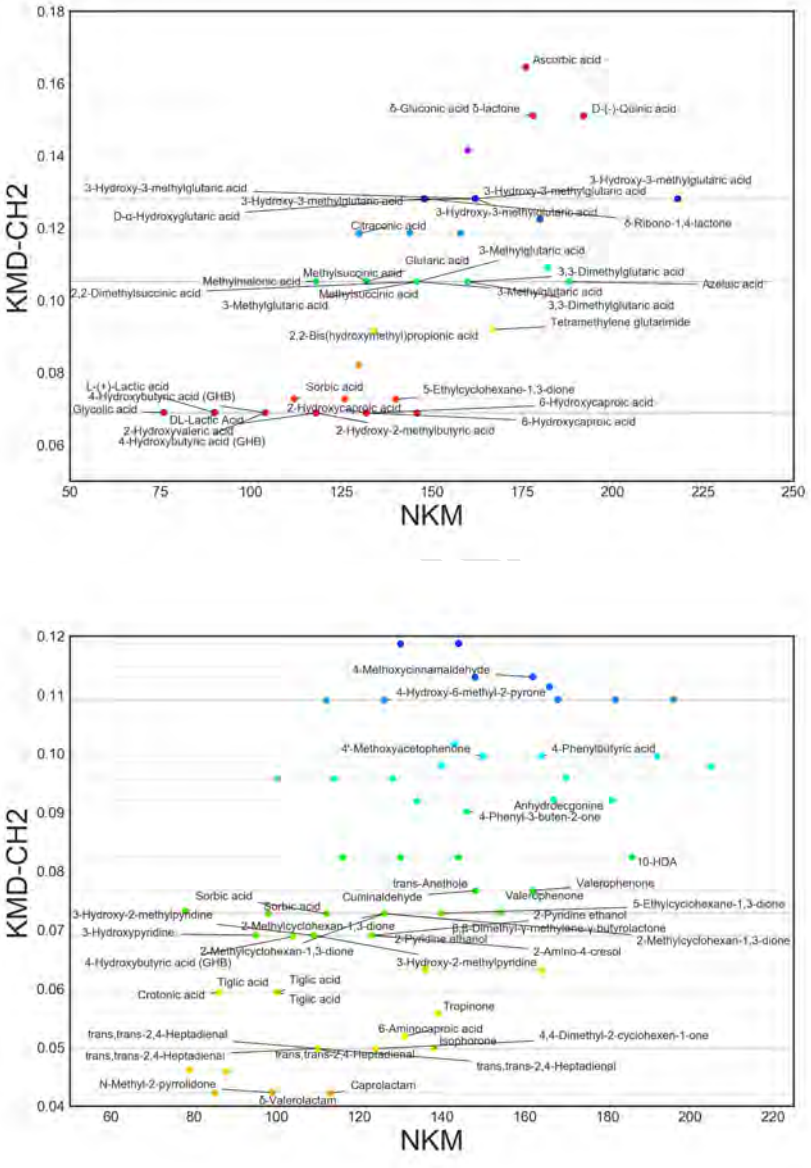

Figure 8: Kendrick plots for the molecular species constituting the core composition of the samples (constant amounts in all the samples regardless of process conditions) with a area threshold of 10^7 for negative (top) and positive (bottom) ESI ionization.

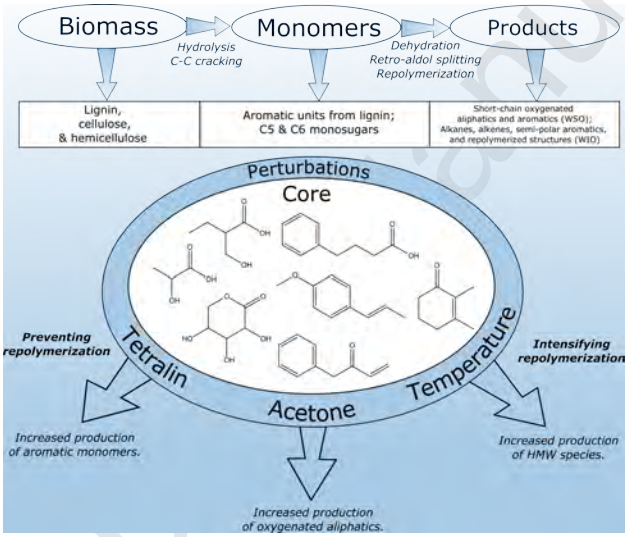

Figure 9: Illustration of the reaction trends at different conditions for biomass conversion clarified by the data mining techniques.

References

[1] J. Akhtar, N. A. S. Amin, A review on process conditions for optimum bio-oil yield in hydrothermal liquefaction of biomass, Renew. Sustain. Energy Rev. 15 (3) (2011) 1615–1624.

[2] N. Akiya, P. E. Savage, Roles of water for chemical reactions in high-temperature water, Chem. Rev. 102 (8) (2002) 2725–2750.

[3] T. H. Pedersen, I. Grigoras, J. Hoffmann, S. S. Toor, I. M. Daraban, C. U. Jensen, S. Iversen, R. B. Madsen, M. Glasius, K. R. Arturi, R. P. Nielsen, E. G. Søgaard, L. A. Rosendahl, Continuous hydrothermal co-liquefaction of aspen wood and glycerol with water phase recirculation, Appl. Energ. 162 (2016) 1034–1041.

[4] R. B. Madsen, E. Lappa, P. S. Christensen, M. M. Jensen, M. Klemmer, J. Becker, B. B. Iversen, M. Glasius, Chemometric analysis of composition of bio-crude and aqueous phase from hydrothermal liquefaction of thermally and chemically pretreated Miscanthus x giganteus, Biomass Bioenerg. 95 (2016) 137–145.

[5] European Commission, Steeper Energy builds industrial scale plant worth € 50.6 million, Available online: `https://ec.europa.eu/easme/en/news/steeper-energy-builds-industrial-scale-plant-worth-506-million`, Accessed on 25 February 2018.

[6] T. H. Pedersen, N. H. Hansen, O. M. Pérez, D. E. V. Cabezas, L. A. Rosendahl, Renewable hydrocarbon fuels from hydrothermal liquefaction: A techno-economic analysis, Biofuel. Bioprod. Bior. ISSN 1932-1031, URL `http://dx.doi.org/10.1002/bbb.1831`.

[7] T. Werpy, G. Petersen, A. Aden, J. Bozell, J. Holladay, J. White, A. Manheim, D. Eliot, L. Lasure, S. Jones, Top value added chemicals from biomass. Volume I-Results of screening for potential candidates from sugars and synthesis gas, Tech. Rep., Department of Energy Washington DC, 2004.

[8] J. E. Holladay, J. F. White, J. J. Bozell, D. Johnson, Top value-added chemicals from biomass-Volume IIResults of screening for potential candidates from biorefinery lignin, Tech. Rep., Pacific Northwest National Laboratory (PNNL), Richland, WA (US), 2007.

[9] L. Shuai, J. Luterbacher, Organic solvent effects in biomass conversion reactions, ChemSusChem 9 (2) (2016) 133–155.

[10] L. Shuai, M. T. Amiri, Y. M. Questell-Santiago, F. Héroguel, Y. Li, H. Kim, R. Meilan, C. Chapple, J. Ralph, J. S. Luterbacher, Formaldehyde stabilization facilitates lignin monomer production during biomass depolymerization, Science 354 (6310) (2016) 329–333.

[11] M. Mosteiro-Romero, F. Vogel, A. Wokaun, Liquefaction of wood in hot compressed water Part 2–Modeling of particle dissolution, Chem. Eng. Sci. 109 (2014) 220–235.

[12] M. Mosteiro-Romero, F. Vogel, A. Wokaun, Liquefaction of wood in hot compressed water: Part 1Experimental results, Chem. Eng. Sci. 109 (2014) 111–122.

[13] A. Bridgwater, D. Meier, D. Radlein, An overview of fast pyrolysis of biomass, Org. Geochem. 30 (12) (1999) 1479–1493.

[14] P. J. Valdez, J. G. Dickinson, P. E. Savage, Characterization of product fractions from hydrothermal liquefaction of Nannochloropsis sp. and the influence of solvents, Energy Fuels 25 (7) (2011) 3235–3243.

[15] P. Biller, R. B. Madsen, M. Klemmer, J. Becker, B. B. Iversen, M. Glasius, Effect of hydrothermal liquefaction aqueous phase recycling on bio-crude yields and composition, Biores. Technol. 220 (2016) 190–199.

[16] S. R. Villadsen, L. Dithmer, R. Forsberg, J. Becker, A. Rudolf, S. B. Iversen, B. B. Iversen, M. Glasius, Development and application of chemical analysis methods for investigation of bio-oils and aqueous phase from hydrothermal liquefaction of biomass, Energy Fuels 26 (11) (2012) 6988–6998.

[17] R. B. Madsen, M. M. Jensen, M. Glasius, Qualitative characterization of solid residue from hydrothermal liquefaction of biomass using thermochemolysis and stepwise pyrolysis-gas chromatography-mass spectrometry, Sus. Energ. Fuel. 1 (10) (2017) 2110–2119.

[18] N. Sudasinghe, B. Dungan, P. Lammers, K. Albrecht, D. Elliott, R. Hallen, T. Schaub, High resolution FT-ICR mass

spectral analysis of bio-oil and residual water soluble organics produced by hydrothermal liquefaction of the marine microalga Nannochloropsis salina, Fuel 119 (2014) 47–56.

[19] K. R. Arturi, H. U. Sokoli, E. G. Søgaard, F. Vogel, S. Bjelić, Recovery of value-added chemicals by solvolysis of unsaturated polyester resin, J. Clean. Prod. 170 (2018) 131–136.

[20] K. R. Arturi, S. Kucheryavskiy, E. G. Søgaard, Performance of hydrothermal liquefaction (HTL) of biomass by multivariate data analysis, Fuel Process. Technol. 150 (2016) 94–103.

[21] A. G. Aguilera, P. Alpert, J. S. Dukes, R. Harrington, Impacts of the invasive plant Fallopia japonica (Houtt.) on plant communities and ecosystem processes, Biol. Invasions 12 (5) (2010) 1243–1252.

[22] K. Van Meerbeek, L. Appels, R. Dewil, A. Calmeyn, P. Lemmens, B. Muys, M. Hermy, Biomass of invasive plant species as a potential feedstock for bioenergy production, Biofuel. Bioprod. Bior. 9 (3) (2015) 273–282.

[23] Z. Hromádková, J. Hirsch, A. Ebringerová, Chemical evaluation of Fallopia species leaves and antioxidant properties of their non-cellulosic polysaccharides, Chem. Pap. 64 (5) (2010) 663–672.

[24] D. Donnez, P. Jeandet, C. Clément, E. Courot, Bioproduction of resveratrol and stilbene derivatives by plant cells and microorganisms, Trends Biotechnol. 27 (12) (2009) 706–713.

[25] W. B. Widayatno, G. Guan, J. Rizkiana, X. Hao, Z. Wang, C. Samart, A. Abudula, Steam reforming of tar derived from Fallopia japonica stem over its own chars prepared at different conditions, Fuel 132 (2014) 204–210.

[26] S. S. Toor, L. Rosendahl, A. Rudolf, Hydrothermal liquefaction of biomass: A review of subcritical water technologies, Energy 36 (5) (2011) 2328–2342, ISSN 03605442.

[27] M. Carrier, A. Loppinet-Serani, C. Absalon, C. Aymonier, M. Mench, Degradation pathways of holocellulose, lignin and α-cellulose from Pteris vittata fronds in sub-and super critical conditions, Biomass Bioenerg. 43 (2012) 65–71.

[28] A. Kruse, T. Henningsen, A. Sinag, J. Pfeiffer, Biomass gasification in supercritical water: influence of the dry matter content and the formation of phenols, Ind. Eng. Chem. Res. 42 (16) (2003) 3711–3717.

[29] S. Karagöz, T. Bhaskar, A. Muto, Y. Sakata, Hydrothermal upgrading of biomass: effect of K_2CO_3 concentration and biomass/water ratio on products distribution, Bioresource Technol. 97 (1) (2006) 90–98.

[30] R. C. Neavel, Liquefaction of coal in hydrogen-donor and non-donor vehicles, Fuel 55 (3) (1976) 237–242.

[31] Z. Fang, T. Sato, R. L. Smith Jr., H. Inomata, K. Arai, J. A. Kozinski, Reaction chemistry and phase behavior of lignin in high-temperature and supercritical water, Bioresource Technol. 99 (9) (2008) 3424–3430.

[32] T. D. H. Nguyen, M. Maschietti, T. Belkheiri, L.-E. Åmand, H. Theliander, L. Vamling, L. Olausson, S.-I. Andersson, Catalytic depolymerisation and conversion of Kraft lignin into liquid products using near-critical water, J. Supercit. Fluid. 86 (2014) 67–75.

[33] Y. He, X. Liang, C. Jazrawi, A. Montoya, A. Yuen, A. J. Cole, N. Neveux, N. A. Paul, R. de Nys, T. Maschmeyer, et al., Continuous hydrothermal liquefaction of macroalgae in the presence of organic co-solvents, Algal Res. 17 (2016) 185–195.

[34] Z. Liu, F. Zhang, Effects of various solvents on the liquefaction of biomass to produce fuels and chemical feedstocks, Energy Convers. Manage. 49 (12) (2008) 3498–3504.

[35] H.-j. Huang, X.-z. Yuan, B.-t. Li, Y.-d. Xiao, G.-m. Zeng, Thermochemical liquefaction characteristics of sewage sludge in different organic solvents, J. Anal. Appl. Pyrol. 109 (2014) 176–184.

[36] S. Sangon, S. Ratanavaraha, S. Ngamprasertsith, P. Prasassarakich, Coal liquefaction using supercritical toluene–tetralin mixture in a semi-continuous reactor, Fuel Process. Technol. 87 (3) (2006) 201–207.

[37] A. Koriakin, H. V. Nguyen, D.-W. Kim, C.-H. Lee, Thermochemical Decomposition of Microcrystalline Cellulose Using Sub-and Supercritical Tetralin and Decalin with Fe_3O_4, Ind. Eng. Chem. Res. 54 (18) (2015) 5184–5194.

[38] K. R. Arturi, M. Strandgaard, R. P. Nielsen, E. G. Søgaard, M. Maschietti, Hydrothermal liquefaction of lignin in near-critical water in a new batch reactor: Influence of phenol and temperature, J. Supercrit. Fluids 123 (2017) 28–39.

[39] K. R. Arturi, K. R. Toft, R. P. Nielsen, L. A. Rosendahl, E. G. Søgaard, Characterization of liquid products from

hydrothermal liquefaction (HTL) of biomass via solid-phase microextraction (SPME), Biomass Bioenerg. 88 (2016) 116–125.

[40] HighChem Ltd., Bratislava, Slovakia, mzCloud - Advanced Mass Spectral Database, Available online: https://www.mzcloud.org/, Accessed on 25 February 2018.

[41] Royal Society of Chemistry, Thomas Graham House, Cambridge, UK, ChemSpider, Available online: http://www.chemspider.com/, Accessed on 25 February 2018.

[42] M. M. Mukaka, A guide to appropriate use of correlation coefficient in medical research, Malawi Med. J. 24 (3) (2012) 69–71.

[43] K. H. Esbensen, D. Guyot, F. Westad, L. P. Houmoller, Multivariate data analysis-in practice: an introduction to multivariate data analysis and experimental design, Multivariate Data Analysis, 2002.

[44] S. Kucheryavskiy, R package for Multivariate Data Analysis, doi:\let\@tempa\bibinfo@X@doi10.5281/zenodo.59547, URL https://doi.org/10.5281/zenodo.59547, 2016.

[45] X. Cui, G. A. Churchill, Statistical tests for differential expression in cDNA microarray experiments, Genome Biol. 4 (4) (2003) 210.

[46] D. W. van Krevelen, Graphical statistical method for the study of structure and reaction processes of coal, Fuel 29 (1950) 269–284.

[47] S. Kim, R. W. Kramer, P. G. Hatcher, Graphical method for analysis of ultrahigh-resolution broadband mass spectra of natural organic matter, the van Krevelen diagram, Anal. Chem. 75 (20) (2003) 5336–5344.

[48] B. P. Koch, T. Dittmar, From mass to structure: an aromaticity index for high-resolution mass data of natural organic matter, Rapid Commun. Mass Sp. 20 (5) (2006) 926–932.

[49] E. Kendrick, A Mass Scale Based on CH2= 14.0000 for High Resolution Mass Spectrometry of Organic Compounds., Anal. Chem. 35 (13) (1963) 2146–2154.

[50] V. Rustamov, K. Abdullayev, E. Samedov, Biomass conversion to liquid fuel by two-stage thermochemical cycle, Energ. Convers. Manage. 39 (9) (1998) 869–875.

[51] J. Russell, R. Miller, P. Molton, Formation of aromatic compounds from condensation reactions of cellulose degradation products, Biomass 3 (1) (1983) 43–57.

[52] M. Tymchyshyn, C. C. Xu, Liquefaction of bio-mass in hot-compressed water for the production of phenolic compounds, Bioresource Technol. 101 (7) (2010) 2483–2490.

[53] R. Bro, A. K. Smilde, Principal component analysis, Anal. Methods 6 (9) (2014) 2812–2831.

[54] I. T. Jolliffe, J. Cadima, Principal component analysis: a review and recent developments, Phil. Trans. R. Soc. A 374 (2065) (2016) 20150202.

[55] T. Parsell, S. Yohe, J. Degenstein, T. Jarrell, I. Klein, E. Gencer, B. Hewetson, M. Hurt, J. Im Kim, H. Choudhari, et al., A synergistic biorefinery based on catalytic conversion of lignin prior to cellulose starting from lignocellulosic biomass, Green Chem. 17 (3) (2015) 1492–1499.

[56] E. L. Schymanski, J. Jeon, R. Gulde, K. Fenner, M. Ruff, H. P. Singer, J. Hollender, Identifying Small Molecules via High Resolution Mass Spectrometry: Communicating Confidence, Environ. Sci. Technol. 48 (4) (2014) 2097–2098.

[57] K. Ramanamurty, G. Salvapathi, Catalytic Cyclocondensation of acetone to isophorone, Indian J. Chem., Sect B 38 (1999) 24–28.

[58] K. Ramanamurty, G. Salvapati, New dimensions on value added aldol chemicals of acetone, J. Sci. Ind. Res. 59 (5) (2000) 339–349.

[59] A. A. Peterson, F. Vogel, R. P. Lachance, M. Fröling, M. J. Antal Jr, J. W. Tester, Thermochemical biofuel production in hydrothermal media: A review of sub-and supercritical water technologies, Energy Environ. Sci. 1 (1) (2008) 32–65.

[60] E. Panisko, T. Wietsma, T. Lemmon, K. Albrecht, D. Howe, Characterization of the aqueous fractions from hydrotreatment

and hydrothermal liquefaction of lignocellulosic feedstocks, Biomass Bioenerg. 74 (2015) 162–171.

[61] Z. Srokol, A.-G. Bouche, A. van Estrik, R. C. Strik, T. Maschmeyer, J. A. Peters, Hydrothermal upgrading of biomass to biofuel; studies on some monosaccharide model compounds, Carbohyd. Res. 339 (10) (2004) 1717–1726.

[62] J. W. Pelley, 2 - Structure and Properties of Biologic Molecules, in: J. W. Pelley (Ed.), Elsevier's Integrated Review Biochemistry (Second Edition), W.B. Saunders, 7 – 18, 2012.

Highlights

- Oxygenated water soluble aliphatics were the most common HTL products.
- High-value carboxylic acids constituted the core resilient to process tailoring.
- Tetralin promoted formation of aromatics through solubilization and scavenging.
- Acetone promoted low molecular weight oxygenates through retro-aldol splitting.

HTL

Fallopia japonica (potential lignocellulosic energy-crop)

+

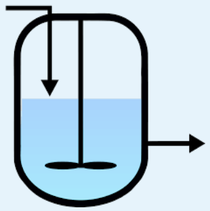

Hydrothermal liqefaction (T, p, t, K_2CO_3, co-solvents)

+

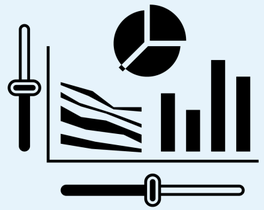

Analytics and data mining strategy

=

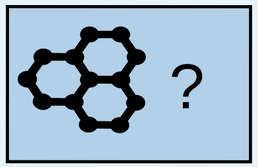

Chemical potential: monomers, fine, building blocks

MOLECULAR COMPOSITION

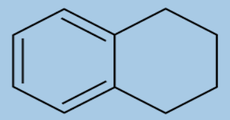

TETRALIN

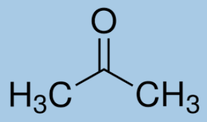

ACETONE

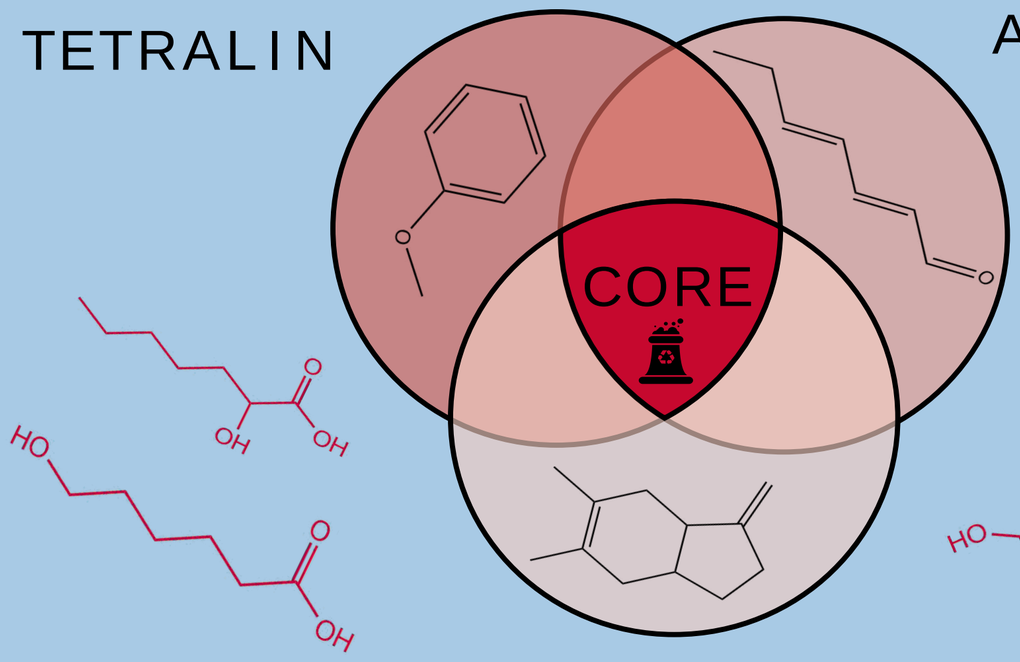

TEMPERATURE (280->300->320 ºC)